Pergamon

Cement and Concrete Research 31 (2001) 983–992

CEMENT AND CONCRETE RESEARCH

Solubility of chromate hydrocalumite ($3CaO{\cdot}Al_2O_3{\cdot}CaCrO_4{\cdot}nH_2O$) 5–75°C

Robert B. Perkins[a], Carl D. Palmer[b,*]

[a]*Department of Geology, Portland State University, P.O. Box 751, Portland, OR 97207-0751 USA*
[b]*Idaho National Engineering and Environmental Laboratory, P.O. Box 1625, MS 2107, Idaho Falls, ID 83415-2107, USA*

Received 2 August 1999; accepted 17 January 2001

Abstract

A secondary precipitate was consistently observed in a series of dissolution and precipitation experiments conducted on synthesized $Ca_6[Al(OH)_6]_2(CrO_4)_3{\cdot}26H_2O$. X-ray diffraction (XRD) patterns, scanning electron microscopy, thermogravimetry, and solid digest analyses demonstrate that d-spacings, crystal morphology, water content, and Ca/Cr/Al ratios for the secondary solid are consistent with chromate hydrocalumite ($3CaO{\cdot}Al_2O_3{\cdot}CaCrO_4{\cdot}15H_2O$). Steady-state aqueous ion concentrations indicate that the experimental aqueous solutions were in apparent equilibrium with both the Cr(VI) analog of ettringite and chromate hydrocalumite. Over the pH range 10.9 to 12.2, the log of the solubility product (log K_{SP}) for the reaction

$$3CaO{\cdot}Al_2O_3{\cdot}CaCrO_4{\cdot}15H_2O \rightleftarrows 4Ca^{2+} + 2Al(OH)_4^- + CrO_4^{2-} + 4OH^- + 9H_2O$$

at 25°C is -30.38 ± 0.28. The temperature dependence of the log K_{SP} obtained from six additional temperatures from 5°C to 75°C is

$$\log K_{SP} = \left(\frac{-2042.1}{T}\right) - 23.480.$$

ΔG_r° and ΔH_r° for the reaction are 173.1 ± 3.7 and 39.1 ± 3.2 kJ mol^{-1} and ΔS_r° is -450 ± 10 J mol^{-1} K^{-1}. Using these values and published partial molal quantities for constituent ions, we calculate $\Delta G_{f,298}^\circ = -9905 \pm 15.7$ kJ mol^{-1}, $\Delta H_f^\circ = -11303 \pm 8.3$ kJ mol^{-1}, and $\Delta S^\circ = 1439 \pm 89$ J mol^{-1} K^{-1} for $3CaO{\cdot}Al_2O_3{\cdot}CaCrO_4{\cdot}15H_2O$.

Keywords: Hydrocalumite; Chromate; Monosulfate; Thermodynamic calculations

1. Introduction

Sulfate hydrocalumite ($3CaO{\cdot}Al_2O_3{\cdot}CaSO_4{\cdot}nH_2O$), also known as calcium aluminum monosulfate or simply "monosulfate," is typically the dominant hydrated calcium alumina-sulfate phase present in mature Portland cement pastes. It is formed as the sulfate concentrations in the pore water decrease due to the formation of early hydration products, primarily ettringite ($Ca_6(Al(OH)_6)_2(SO_4)_3{\cdot}26H_2O$). The ettringite then reacts with tricalcium aluminate ($Ca_3Al_2O_6$), one of the primary clinker phases, to form the more sulfate-depleted sulfate hydrocalumite [1,2]. Both sulfate hydrocalcumite and ettringite are known to allow ionic substitution, including Fe^{3+} and Cr^{3+} for the Al^{3+} and OH^-, CO_3^{2-}, SeO_4^{2-}, and CrO_4^{2-} for SO_4^{2-} [1–7]. The widespread use of cement and concrete and the ability of hydrocalumite to structurally incorporate toxic ions makes it important with regard to the mobility of pollutants in the environment, remediation of contaminated sites, and waste immobilization in cementitious materials.

Substitution of hexavalent chromium in hydrocalumite is of particular interest as chromium is a widespread pollutant that is acutely toxic, teratogenic, mutagenic, and carcinogenic [8–11]. Chromium is a frequently cited contaminant at hazardous waste sites and may be found in several alkaline environments including naturally alkaline soils, fly ash, cement and concrete, chromite ore processing wastes, and basic waste mixtures. In alkaline solutions, hexavalent chromium primarily occurs as CrO_4^{2-}. The identical charge,

* Corresponding author. Tel.: +1-208-526-4478; fax: +1-208-526-0875.
E-mail address: palmcd@inel.gov (C.D. Palmer).

0008-8846/01/$ – see front matter
PII: S0008-8846(01)00507-5

similar structure, and comparable thermochemical radii of CrO_4^{2-} and SO_4^{2-} suggest that chromate should readily substitute in the crystal structure of hydrocalumite. Palmer [12] identified CrO_4-bearing ettringite and a nearly pure chromate hydrocalumite ($3CaO{\cdot}Al_2O_3{\cdot}CaCrO_4{\cdot}nH_2O$) phase in samples of concrete contaminated by chrome-laden solutions. Such observations demonstrate the potential importance of these phases in controlling the fate and transport of hexavalent chromium in alkaline environments. However, we are unaware of any published solubility data for chromate hydrocalumite.

The purpose of this study is to determine the solubility product (K_{SP}) of $3CaO{\cdot}Al_2O_3{\cdot}CaCrO_4{\cdot}nH_2O$ from 5°C to 75°C. Thermodynamic properties for this phase are calculated from this information. The results of this study should be useful to workers dealing with chromium migration, waste immobilization in alkaline environments, and chromium–cement interactions.

2. Background

The formation of sulfate hydrocalumite from tricalcium aluminate ($Ca_3Al_2O_6$) and gypsum ($CaSO_4{\cdot}2H_2O$) in water is often assumed to occur in two stages. In the first step, hydration of $Ca_3Al_2O_6$ in the presence of gypsum yields ettringite (Eq. (1)):

$$Ca_3Al_2O_6 + 3(CaSO_4{\cdot}2H_2O) + 26H_2O \rightleftarrows Ca_6(Al(OH)_6)_2(SO_4)_3{\cdot}26H_2O. \quad (1)$$

As the aqueous sulfate concentrations decrease and the hydration of $Ca_3Al_2O_6$ continues, the ettringite is converted to sulfate hydrocalumite:

$$Ca_6(Al(OH)_6)_2(SO_4)_3{\cdot}26H_2O + 2Ca_3Al_2O_6 + 4H_2O \rightleftarrows 3(3CaO{\cdot}Al_2O_3{\cdot}CaSO_4{\cdot}12H_2O). \quad (2)$$

We used the most commonly cited hydration number, 12, in Eq. (2). However, the degree of hydration of sulfate hydrocalumite is variable and largely depends on the relative humidity of the atmosphere in contact with the solid and the ionic strength of the solution [1]. Differing hydration states alter some d-spacings and Lea [1] lists the characteristic d-spacings for sulfate hydrocalumites with 7, 10, 12, and 15 waters of hydration. Kuzel [13] determined 14 waters of hydration based on X-ray diffraction (XRD) analyses of sulfate hydrocalumite in the presence of water. Changes in the hydration are generally reversible [1].

3. Methods

The results discussed in the following sections are based on continued interpretation of data obtained from our earlier study of $Ca_6[Al(OH)_6]_2(CrO_4)_3{\cdot}26H_2O$ solubility as well as additional characterization of solid residues obtained in that study. The specific methodology for synthesis and characterization of the initial solid, dissolution and precipitation experiments, and analyses of the resulting solutions are detailed in our previously published paper [14].

Equilibrium with chromate hydrocalumite was achieved by equilibrating solutions with $Ca_6[Al(OH)_6]_2(CrO_4)_3{\cdot}26H_2O$ which was synthesized from suspensions of $3CaO{\cdot}Al_2O_3$ and $CaCrO_4$ using a modification of a method described by Odler and Abdul-Maula [2]. Both dissolution and precipitation experiments were conducted on the chromate ettringite at 25°C in high-density polyethylene (HDPE) bottles using N_2-purged solutions. Solutions were prepared in a glove box equipped with a CO_2-scrubber. HDPE bottles were sealed in glass mason jars before removing them from the chamber. The jars were kept in a water bath at a constant temperature (±0.3°C) for a minimum of 14 days, well after the 2 days required to attain steady-state concentrations of analytes. Precipitation of chromate ettringite was induced by spiking the suspensions remaining at the conclusion of dissolution experiments with 7 to 7.5 ml of 70 mM $Ca(NO_3)_2$. All other aspects of the chromate ettringite precipitation experiments were identical to the dissolution experiments. All of the experiments are precipitation experiments with respect to chromate hydrocalumite. In addition to the experiments conducted at 25°C, a series of experiments were conducted at 5°C, 15°C, 35°C, 45°C, 60°C, and 75°C.

The pH measurements were made within the glove box at the time of sampling. The meter was calibrated using pHydrion 7.00, 10.00, and 12.00 buffers. The samples were filtered through 0.45-μm polysulfone membrane filters. Samples intended for cation analysis were preserved with HNO_3 (0.5% solution). Ca and Al were analyzed by atomic absorption spectroscopy using a lanthanum matrix modifier. Cr(VI) was analyzed colorimetrically using the diphenylcarbizide method [15] and measuring the absorbance at 540 nm on a Beckman DU 640 spectrophotometer. Powder XRD analyses of the solids that were present at the end of the experiments were obtained using CuKα radiation on a Norelco XRG 3000 unit.

Solid-phase characterizations of the initial $Ca_6[Al(OH)_6]_2(CrO_4)_3{\cdot}26H_2O$ are discussed by Perkins and Palmer [14]. Experimental residues were analyzed via XRD. Additional solid characterizations were performed on select experimental residues, including thermogravimetric analyses (TGA) to measure the degree of hydration and chemical analyses of the solid dissolved in dilute nitric acid to measure the stoichiometry of the solid residues. The morphology and size of crystallites were assessed using imaging with a Phillips XL30 environmental scanning electron microscope (ESEM) using an accelerating voltage of 10 kV. Samples were sputter coated with ~100 Å of Au–Pd prior to imaging. Composition of the crystallites was obtained with a Princeton Gamma Tech IMIX energy dispersive X-ray spectrometer (EDX) at a working distance of 10 mm. Quantification with EDX was done using a

standardless ZAF technique [16] using the ZAF-4 software package provided by the manufacturer of the X-ray unit.

4. Results and discussion

The concentrations of Ca, Al, and Cr(VI) obtained from solutions equilibrated with synthesized $Ca_6[Al(OH)_6]_2(CrO_4)_3\cdot 26H_2O$ are presented in Perkins and Palmer [14]. The stoichiometry of these solutions was found to differ from that of the initial solid, indicating the formation of a secondary precipitate.

4.1. Powder XRD

XRD patterns of solid residues from the dissolution experiments show seven peaks not observed in the initial solid. These peaks were attributed to the secondary precipitate. Specifically, the XRD patterns (Table 1) show a decrease in the relative intensity of the {100} $Ca_6[Al(OH)_6]_2(CrO_4)_3\cdot 26H_2O$ peak (d-spacing of 9.87 Å) and the appearance of a prominent peak at 10.21–10.27 Å. The {110} peak (5.03–5.06 Å) is also diminished and a new peak having maximum intensity appears at ~5.07–5.18 Å. Unit cell dimensions were calculated for all residues, both with and without the 10.21–10.27 and 5.07–5.18 Å peaks. Residual errors for the 10.21 and 10.27 Å peaks were higher than the errors calculated for the other peaks, exceeding 0.1 Å.

Myneni [17] also observed a diminished {100} peak and the appearance of a new peak at 10.33 Å when Cr(VI) concentrations exceeded 1.29 mM in coprecipitation experiments conducted with sulfate ettringite. Myneni [17] notes that the slightly larger radius of CrO_4^{2-} over SO_4^{2-} does not adequately explain the increase in d-spacing to 10.33 Å.

The discrepancies observed in our XRD results can be explained by the formation of chromate hydrocalumite. The coexistence of chromate hydrocalumite and the Cr(VI) analog of ettringite is expected as mixtures of sulfate hydrocalumite and ettringite are known to form when the $CaSO_4/Al_2O_3$ ratio exceeds unity [1]. Palmer [12] observed a Cr(VI)-bearing ettringite phase together with an almost pure chromate hydrocalumite phase in samples of concrete which had been contaminated with chromium-laden solutions.

There are few published XRD patterns for chromate hydrocalumite. However, the XRD patterns of sulfate and chromate hydrocalumites may be expected to be comparable given the minor difference (0.1 Å) in ionic radii of sulfate and chromate. An additional complication is that hydrocalumite phases exhibit variable hydration states, each having a different X-ray pattern. Lea [1] lists 10.3, 5.15, 4.03, and 2.87 Å d-spacings for sulfate hydrocalumite with 15 water molecules ($3CaO\cdot Al_2O_3\cdot CaSO_4\cdot 15H_2O$). Two of these d-spacings correspond well with major peaks (~10.27, 5.15 Å) that appeared in the XRD patterns of the experimental residues but not in the initial solid. A third peak (2.87 Å) was noted but was also present in the initial synthesized solid XRD pattern.

The PDF pattern 44-0602 for $Ca_4Al_2SO_{10}\cdot 16H_2O$ lists d-spacings of 10.23, 5.11, 3.41, 2.56, and 2.04 Å. The first four of these d-spacings correspond to XRD peaks (10.21–10.27, 5.07–5.18, 3.38–3.44, and 2.53 Å) obtained for the experimental residues but which were not observed in XRD patterns for the initial synthesized solid. The relative intensity of the fifth peak is only 4% and so the corresponding peak in our XRD pattern may not be distinguishable from the background.

A maximum peak having a d-spacing of 4.83 Å was obtained for one sample (12.5 pH). However, hydrocalumite planar spacings perpendicular to the *c*-axis are particularly dependent on the degree of hydration. Values between 4.2 and 5.12 Å have been observed for the {006} peak for $Ca_4Al_2CrO_{10}\cdot nH_2O$ with *n* equal to 9, 12, and 14 waters (personnel communication obtained in review).

Three additional peaks were noted in XRD patterns of experimental residues but were not observed in the initial synthesized solid. Two of these peaks (~3.87 and 2.29 Å) match peaks ({110} and {205}, respectively) reported for $Ca_4Al_2CrO_{10}\cdot 12H_2O$ in PDF file 41-0478. The third (3.04 Å) corresponds to the {107} peak (3.03 Å) listed for sulfate hydrocalumite ($Ca_4Al_2SO_{10}\cdot 12H_2O$) in PDF file 18-0275.

4.2. Additional solid characterization

The peaks associated with the secondary phase dominate the XRD pattern of the highest pH samples. The XRD pattern for the "12.5" pH sample displays neither the {100} nor the {110} ettringite peak and is missing nearly all of the other peaks characteristic of $Ca_6[Al(OH)_6]_2(CrO_4)_3\cdot 26H_2O$ (Table 1). Therefore, the "12.5" pH samples were not included in subsequent calculations of the solubility product for $Ca_6[Al(OH)_6]_2(CrO_4)_3\cdot 26H_2O$ [14].

A larger volume $Ca_6[Al(OH)_6]_2(CrO_4)_3\cdot 26H_2O$ suspension was prepared using a NaOH solution with pH >12.5 in an effort to obtain a relatively pure sample of the secondary phase for further solid characterization. Although the XRD pattern for the resulting solid material is clearly dominated by the secondary solid peaks, minor peaks characteristic of the original $Ca_6[Al(OH)_6]_2(CrO_4)_3\cdot 26H_2O$ were noted (e.g., the {110} peak was present, but with a relative intensity of ~1% rather than 100% as noted for the initial synthesized solid; Table 1). One additional peak (5.32 Å), not observed in previous patterns, was present with a relative intensity of 7%. The d-spacing does closely match the {004} chromate ettringite peak; however, this is unlikely given the small relative intensity of the {110} chromate ettringite peak. The 5.32 Å peak more likely represents the {006} chromate hydrocalumite peak; although the d-spacing is >0.1 Å larger than previously listed values, the d-spacing would be expected to be larger in crystallites with a greater number of waters of hydration.

Table 1
Comparison of powder XRD peaks from initial synthetic $Ca_6[Al(OH)_6]_2(CrO_4)_3{\cdot}26H_2O$ with PDF patterns and select experimental residues

	PDF 44-0602[b]		PDF 41-0218[c]		Initial synthesized Cr(VI)-ettringite		Solid filtrate 25°C, pH 10.5 precipitation experiment		Solid filtrate 25°C, pH 12.0 dissolution experiment		Solid filtrate 25°C, pH 12.5 dissolution experiment		Solid filtrate 75°C, pH 10.5 dissolution experiment		Solid filtrate 25°C, pH 12.5 synthesis	
h,k,l[a]	d (Å)	*I*	d (Å)	*I*	d (Å)	*I*	d (Å)	*I*	d (Å)	*I*	d (Å)	*I*	d (Å)	*I*	d (Å)	*I*
002	–	–	*10.73*	*5*	–	–	–	–	–	–	–	–	–	–	–	–
H003	10.23	100	–	–	–	–	10.21	83	10.21	68	10.27	53	10.10	97	10.20	46
100	–	–	9.87	100	9.87	74	9.87	27	–	–	–	–	9.87	32	–	–
101	–	–	8.97	14	8.93	10	–	–	–	–	–	–	–	–	–	–
102	–	–	7.27	4	–	–	–	–	–	–	–	–	–	–	–	–
103	–	–	5.79	18	–	–	–	–	–	–	–	–	–	–	–	–
110	–	–	5.61	80	5.73	100	5.69	20	5.71	1	–	–	–	–	5.75	1
??	–	–	–	–	–	–	–	–	–	–	–	–	–	–	5.32	7
H006	5.11	93	–	–	–	–	5.18	100	5.08	100	4.83	100	5.15	100	5.07	100
112	–	–	5.03	23	5.06	55	5.05	11	–	–	–	–	–	–	–	–
200	–	–	4.93	5	–	–	–	–	–	–	–	–	–	–	–	–
104	–	–	4.714	50	4.73	45	4.72	2	–	–	–	–	–	–	4.74	7
202	–	–	4.482	1	4.46	10	–	–	4.48	5	4.49	1	–	–	4.485	16
H007	–	–	–	–	–	–	–	–	–	–	–	–	–	–	4.390	2
203	–	–	4.062	11	4.08	12	–	–	–	–	–	–	–	–	–	–
105	–	–	3.936	10	–	–	–	–	–	–	–	–	–	–	–	–
114	–	–	3.905	70	3.92	81	3.91	8	–	–	–	–	–	–	–	–
H105	–	–	–	–	–	–	3.86	5	3.87	2	3.88	2	3.87	8	3.870	11
210	–	–	3.729	5	3.74	7	3.72	2	–	–	–	–	–	–	3.763	2
204	–	–	3.632	7	3.64	10	–	–	–	–	–	–	–	–	–	–
212	–	–	3.523	27	3.53	45	3.50	7	3.55	11	3.56	3	–	–	3.555	23
H009	3.407	46	–	–	–	–	3.44	27	3.37	11	3.38	5	3.44	28	3.374	10
213	–	–	3.308	8	–	–	–	–	–	–	–	–	–	–	–	–
300	–	–	3.290	21	3.29	43	3.28	6	–	–	–	–	–	–	3.249	3
H108	–	–	–	–	3.04	10	3.04	46	3.04	12	3.05	7	3.04	62	3.044	65
116	–	–	3.030	7											–	–
220	–	–	2.848	1	2.87	7	2.87	5	2.88	7	2.87	2	2.88	18	2.882	17
304	–	–	2.804	45	2.80	34	2.80	8	2.79	6	2.79	4	–	–	2.792	9
310	–	–	2.737	7	2.74	10	2.74	5	–	–	–	–	–	–	–	–
008	–	–	2.684	10	2.68	9	–	–	–	–	–	–	–	–	–	–
312	–	–	2.651	15	2.65	26	2.65	10	–	–	–	–	–	–	–	–
216	–	–	2.582	45	2.58	64	2.59	3	–	–	–	–	2.59	13	–	–
313	–	–	2.557	4	–	–	–	–	–	–	–	–	–	–	–	–
H116	2.556	15	2.524	6	–	–	–	–	2.53	6	2.53	6	–	–	2.526	4
224	–	–	2.516	4	–	–	–	–	–	–	–	–	–	–	–	–
400	–	–	2.466	1	2.50	17	2.49	10	2.50	11	2.51	4	2.50	20	2.503	30
314	–	–	2.438	5	–	–	–	–	–	–	–	–	–	–	–	–
118	–	–	2.428	5	2.43	10	–	–	2.42	6	2.42	2	–	–	2.422	14
208	–	–	2.358	5	2.36	5	–	–	–	–	–	–	–	–	–	–
H105	–	–	–	–	–	–	2.29	12	2.29	2	–	–	2.29	17	–	–
320	–	–	2.264	8	2.26	17	2.26	5	2.25	21	–	–	–	–	–	–
226	–	–	2.229	40	2.23	79	2.23	8	–	–	–	–	–	–	–	–
322	–	–	2.215	7	–	–	–	–	–	–	–	–	–	–	–	–
316	–	–	2.174	23	2.17	41	2.17	4	–	–	–	–	–	–	–	–
323	–	–	2.158	4	2.15	17	2.15	3	–	–	–	–	–	–	–	–
410	–	–	2.153	4	2.11	7	–	–	–	–	–	–	–	–	–	–
412	–	–	2.111	2	2.09	2	2.09	9	–	–	–	–	2.10	13	–	–

I = relative intensity (I/I_{max}).

[a] "H###" denotes peak assigned to hydrocalumite ($3CaO{\cdot}Al_2O_3{\cdot}CaCrO_4{\cdot}nH_2O$); d-spacings highly dependent on degree of hydration. Other hkls from PDF 41-0218.

[b] Powder diffraction file for $Ca_4Al_2SO_{10}{\cdot}16H_2O$.

[c] PDF for $Ca_6[Al(OH)_6]_2(CrO_4)_3{\cdot}26H_2O$. Peaks with d-spacings < 2.11 Å excluded.

TGA was conducted on the solid residue from this larger suspension. A 2.3 mg sample was heated from 40°C to 900°C at a constant rate of 10°C/min using a Perkin Elmer TGA 7 analyzer. Comparison of the resulting mass-loss curve with that of the initial solid shows that mass loss occurs in four rather than three intervals as was the case for $Ca_6[Al(OH)_6]_2(CrO_4)_3{\cdot}26H_2O$ (Fig. 1). The total percentage mass loss at 900°C, 39.0%, is close to the expected

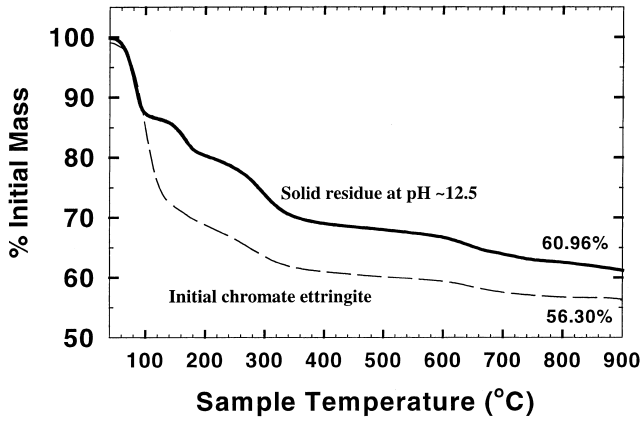

Fig. 1. Thermogravimetric mass fraction plots for initial synthesized $Ca_6[Al(OH)_6]_2(CrO_4)_3{\cdot}26H_2O$ (dashed) and solid residues from experiments at initial pH >12.5 (solid).

value of 38.8% for $3CaO{\cdot}Al_2O_3{\cdot}CaSO_4{\cdot}15H_2O$ and significantly less than the expected mass loss of 43.8% for $Ca_6[Al(OH)_6]_2(CrO_4)_3{\cdot}26H_2O$.

Replicate portions ($\sim$7 mg) of solid were digested in dilute nitric acid and analyzed for Ca, Al, and Cr(VI) using the same techniques as for aqueous samples. The resulting stoichiometry, normalized to Al, is 4.26($\pm$0.02):2.00:1.28($\pm$0.04) (Ca/Al/Cr) compared to an ideal stoichiometry of 4.00:2.00:1.00 for pure chromate hydrocalumite. Thus, the chemical digest data suggest an apparent excess of Ca and Cr. The excess may be either $CaCrO_4$ precipitated from the evaporation of residual water or it could be explained by the presence of 14% chromate ettringite. The latter hypothesis is consistent with the observation of ettringite peaks in the XRD spectra. Thus, the results of the thermogravimetry, powder XRD, and the solid digest analysis are consistent with a $3CaO{\cdot}Al_2O_3{\cdot}CaSO_4{\cdot}15H_2O$ containing $<$15 wt.% $Ca_6[Al(OH)_6]_2(CrO_4)_3{\cdot}26H_2O$.

SEM images of the residue from the pH "12.5" suspension showed the material to be comprised of hexagonal platelets $\sim$1 to 10 μm in diameter (Fig. 2). The hexagonal form of the plates is consistent with the morphology reported for hydrocalumite (1, 7, 12). The average of 5 EDX spectra normalized to Al yielded Ca/Al/Cr ratios of 5.08($\pm$0.46):2.00:2.14($\pm$0.32) which suggests excess Ca and Cr(VI) associated with the crystallites. The amount of excess Ca and Cr is greater than that obtained in the bulk chemical analysis suggesting that the excess Ca and Cr is associated more with the surfaces of the crystallites, possibly including $CaCrO_4$ residues formed during drying of filtered solids.

Based on the analogy with the $Ca-Al-SO_4-H_2O$ system, the observations of chromate hydrocalumite and a Cr(VI)-analog of ettringite in chromium-contaminated concrete, the correspondence of secondary XRD peaks with available sulfate and chromate hydrocalumite XRD patterns, the crystal morphology determined by SEM, and the results of TGA and solid digest analyses of residues, we have identified the secondary phase as chromate hydrocalumite with 12 to 16 waters of hydration.

The stability of ion concentrations over time suggests that equilibrium was achieved in our experiments. The presence of the peaks for both the chromate ettringite and chromate hydrocalumite in all samples with pH $<$12.5 suggests that equilibrium is attained with both phases. For the "12.5" pH samples, the ion activity products (IAPs) calculated for the dissolution of the chromate analog of ettringite were significantly lower than those calculated for the other samples. The low IAPs and decidedly uncharacteristic XRD patterns obtained for these samples indicate that they were equilibrated only with the chromate hydrocalumite phase.

The relative intensities of the chromate hydrocalumite XRD peaks increase with the temperature of the dissolution experiment. Peaks corresponding to 10.10 and 5.15 Å for chromate hydrocalumite are so dominant in the XRD pattern obtained for 75°C dissolution samples that many chromate ettringite peaks may be obscured (Table 1). However, a peak at 9.87 Å having a relative intensity of 32% matches the {100} peak determined for the initial synthesized solid, again indicating both phases were present. An increase in

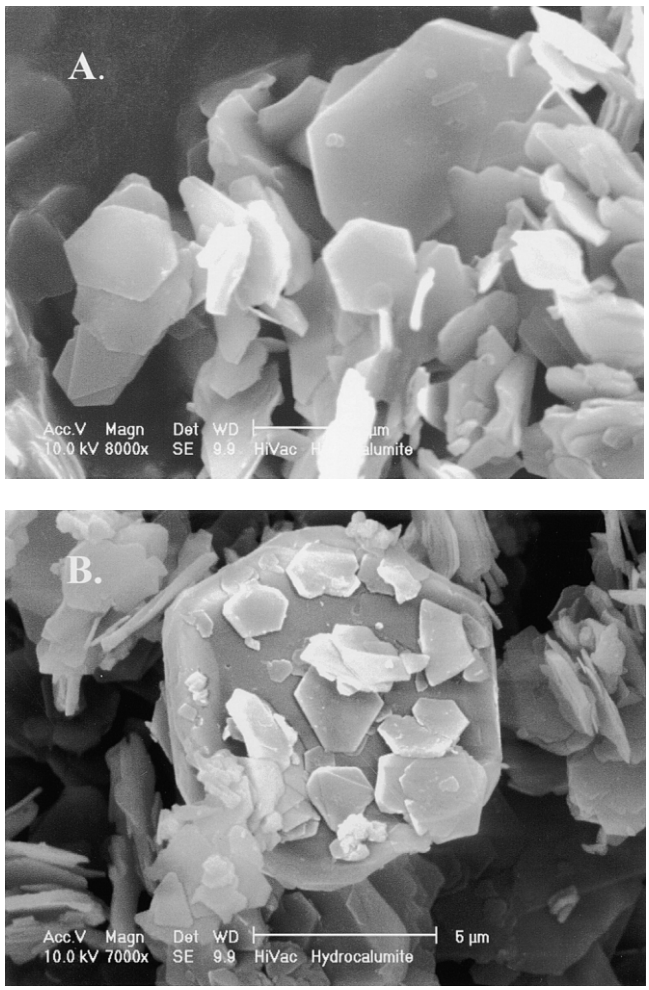

Fig. 2. SEM images of hexagonal crystallites observed in the residue of the pH "12.5" experiment.

Table 2
Thermodynamic data used to update MINTEQA2 databases

Reactions	kJ mol^{-1}		J mol^{-1} K^{-1}			
	ΔG_r°	ΔH_r°	ΔS_r°	ΔC_P	log K_{SP}	Source[a]
$H_2O - H^+ = OH^-$	79.85	55.81	− 80.66	− 212.5	− 13.99	[21,22]
Aqueous species						
$CrO_4^{2-} + 2H^+ = H_2CrO_4^0$	− 39.8	− 26.0	85	–	6.97	[23]
$CrO_4^{2-} + H^+ = HCrO_4^-$	− 37.2	6.0	185	–	6.52	[23]
$2CrO_4^{2-} + 2H^+ - H_2O = Cr_2O_7^{2-}$	− 97.2	− 25.54	145	–	17.01	[21,23]
$Ca^{2+} + CrO_4^{2-} = CaCrO_4^0$	− 15.81	–	–	–	2.77	[14]
$Ca^{2+} + H_2O - H^+ = CaOH^+$	73.22	77.47	14.6	− 38.0	− 12.83	[21,22]
$Al^{3+} + H_2O = AlOH^{2+} + H^+$	28.35	55.73	91.0	0.65	− 4.97	[21,24]
$Al^{3+} + 2H_2O = Al(OH)^{2+} + 2H^+$	57.70	122.6	218	− 225	− 10.11	[21,24]
$Al^{3+} + 3H_2O = Al(OH)_3^0 + 3H^+$	95.15	176.4	–	–	− 16.67	[21,24]
$Al^{3+} + 4H_2O = Al(OH)_4^- + 4H^+$	131.3	181.4	167.7	− 91.8	− 23.00	[21,24]
Solid phases						
$Ca(OH)_2 = Ca^{2+} + 2H_2O - 2H^+$	− 129.6	− 129.6	0.02	31.71	22.70	[21,22,26]
$Al_2O_{3,\ corundum} = 2Al^{3+} + 3H_2O - 6H^+$	− 96.63	− 243.6	− 491	− 125	16.93	[21,24]
$Al_2O_{3,\ \gamma\text{-Alumina}} = 2Al^{3+} + 3H_2O - 6H^+$	− 104.6	− 265.9	− 533	− 93.0	18.33	[21,24]
$Al(OH)_{3,\ amph} = Al^{3+} + 3H_2O - 3H^+$	− 61.65	− 110.8	–	–	10.8	[27]
$AlOOH,\ _{boehemite} = Al^{3+} + 2H_2O - 3H^+$	− 43.60	− 116.2	− 243	− 23.5	7.64	[21,22,25]
$AlOOH,\ _{diaspore} = Al^{3+} + 2H_2O - 3H^+$	− 40.00	− 112.0	− 241	− 22.4	7.01	[21,22,25]
$Al(OH)_{3,\ gibbsite} = Al^{3+} + 3H_2O - 3H^+$	− 44.26	− 105.3	− 205	14.3	7.75	[21,22,25]
$Ca_6[Al(OH)_6]_2(CrO_4)_3{\cdot}26H_2O = 6Ca^{2+} + 2Al(OH)^{4-} + CrO_4^{2-} + 4OH^- + 26H_2O$	236.6 ± 3.9	77.5 ± 2.4	− 534 ± 83	− 1510 ± 140	− 41.5 ± 0.30	[14]
$3CaO{\cdot}Al_2O_3{\cdot}CaCrO_4{\cdot}15H_2O = 4Ca^{2+} + 2Al(OH)_4^- + CrO_4^{2-} + 4OH^- + 15H_2O$	173.1 ± 3.7	39.1 ± 3.2	− 450 ± 10		− 30.38 ± 0.28	This Study

[a] Multiple numbers indicate sources for individual ion or solid phase data that were used in calculating data presented.

the relative mass of chromate hydrocalumite with increasing temperature is to be expected. Indeed, one method for synthesis of sulfate hydrocalumite is to heat a suspension of ettringite to 100°C [18].

4.3. Dissolution and precipitation experiments

As previously noted, the observed molar ratios of ions in solution [14] do not agree with the ideal or measured

Table 3
Calculated activities and IAPs for the chromate hydrocalumite phase in experiments conducted at 25°C

Sample batch	Measured pH	log $\{Ca^{+2}\}$	log $\{Al(OH)_4^-\}$	log $\{CrO_4^{2-}\}$	log $\{OH^-\}$	log $\{Na^+\}$	Ionic strength (m)	Charge balance error (%)[a]	Log (IAP)
25°C dissolution samples									
25-10.5	11.04 ± 0.04	− 2.63	− 2.72	− 2.83	− 2.96	− 3.07	0.0147	3.12	− 30.63 ± 0.10
25-11.0	11.14 ± 0.02	− 2.68	− 2.80	− 2.80	− 2.86	− 2.85	0.0145	1.03	− 30.53 ± 0.12
25-11.5	11.35 ± 0.04	− 2.80	− 3.01	− 2.78	− 2.65	− 2.47	0.0144	± 1.53	− 30.59 ± 0.03
25-11.5r	11.42 ± 0.02	− 2.74	− 3.23	− 2.79	− 2.58	− 2.48	0.0150	4.54	− 30.55 ± 0.07
25-12.0	11.85 ± 0.03	− 2.85	− 3.74	− 2.91	− 2.15	− 2.05	0.0186	8.99	− 30.36 ± 0.01
25-12.0r	11.62 ± 0.04	− 2.39	− 4.01	− 3.20	− 2.38	− 1.82	0.0352	< 1%	− 30.28 ± 0.04
25-12.5	12.13 ± 0.01	− 2.46	− 4.88	− 3.30	− 1.87	− 1.67	0.0539	< 1%	− 30.39 ± 0.01
25°C precipitation samples									
P25-10.5	10.90 ± 0.03	− 2.12	− 2.98	− 3.37	− 3.09	− 3.26	0.0558	− 4.98	− 30.19 ± 0.02
P25-10.5r	10.97 ± 0.06	− 2.18	− 3.12	− 3.40	− 3.03	− 3.58	0.0480	− 7.47	− 30.49 ± 0.25
P285-11.5	11.14 ± 0.01	− 2.11	− 3.29	− 3.40	− 2.86	− 2.61	0.0580	± 1.86	− 29.89 ± 0.02
P25-11.5r	11.30 ± 0.01	− 2.19	− 3.61	− 3.41	− 2.70	− 2.55	0.0484	− 3.53	− 30.19 ± 0.08
P25-12.0	11.54 ± 0.06	− 2.17	− 3.98	− 3.44	− 2.46	− 2.19	0.0568	− 1.98	− 29.92 ± 0.01
P25-12.5	12.15 ± 0.01	− 2.22	− 5.52	− 3.50	− 1.84	− 1.71	0.0707	0.94	− 30.82 ± 0.18

"Dissolution" and "precipitation" refer to chromate ettringite. All of the experiments are precipitation experiments with respect to chromate hydrocalumite.

[a] Charge balance error

$$= \frac{\sum_{\text{cations}} z_i c_i - \sum_{\text{anions}} z_j c_j}{\sum_{\text{cations}} z_i c_i + \sum_{\text{anions}} z_j c_j} \times 100$$

Positive values indicate excess cations, negative values indicate excess anions; ± indicates both excess cations and anions within sample replicates.

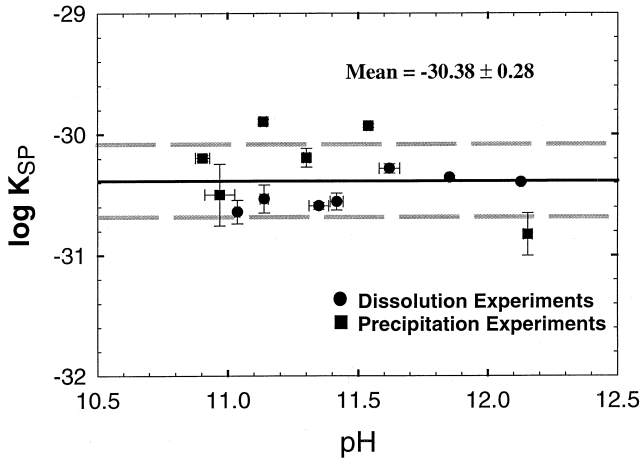

Fig. 3. Calculated IAPs versus pH for the chromate hydrocalumite phase from 25°C "dissolution" and "precipitation" experiments. Dashed lines represent one standard deviation from the overall mean log K_{SP}. "Dissolution" and "precipitation" refer to chromate ettringite. All the experiments are precipitation experiments with respect to chromate hydrocalumite.

solid stoichiometry of $Ca_6[Al(OH)_6]_3(CrO_4)_3{\cdot}26H_2O$. The excess CrO_4^{2-} in solution is consistent with the precipitation of chromate hydrocalumite which would preferentially remove a greater fraction of Ca and Al from solution. The diminished Al concentrations observed in the higher pH samples may be the result of precipitation of aluminum hydroxides or oxyhydroxides. Solutions with pH > 11.35 are near saturation with respect to boehmite, diaspore, and gibbsite.

Aqueous activities for Ca^{2+}, $Al(OH)_4^-$, and CrO_4^{2-} as well as Na^+ and NO_3^- (the latter from $Ca(NO_3)_2$ spikes added to induce precipitation) were calculated with the geochemical speciation model MINTEQA2 [19]. Individual ion activity coefficients, γ_i, were calculated using the Davies Equation (Eq. (3)):

$$\log\gamma_i = -AZ_i^2\left(\frac{\sqrt{I}}{1+\sqrt{I}} - 0.24I\right) \quad (3)$$

where A is the Debey–Huckel parameter which is equal to 0.5092 at 25°C and 1 bar total pressure, Z_i is the charge on the particular ion, i, and I is the ionic strength of the solution.

The databases used by MINTEQA2 were first modified to include pertinent, updated thermodynamic data from available literature (Table 2). IAPs for the dissolution reaction

$$3CaO{\cdot}Al_2O_3{\cdot}CaCrO_4{\cdot}15H_2O \rightleftarrows 4Ca^{2+} + 2Al(OH)_4^- + CrO_4^{2-} + 4OH^- + 9H_2O \quad (4)$$

were calculated from the activities using

$$IAP = \{Ca^{+2}\}^4\{Al(OH)_4^-\}^2\{CrO_4^{2-}\}\{OH^-\}^4\{H_2O\}^9 \quad (5)$$

At equilibrium, the IAP equals the solubility product, K_{SP}. The log IAPs calculated for all 25°C samples (Table 3) vary by less than one log unit from −30.83 to −29.89 (Fig. 3). The maximum value is associated with a sample with pH near the midrange of values. Although the lowest value is associated with the highest pH (12.15), the sample with the next highest pH (12.13) has a corresponding log IAP (−30.39) very near the average value of −30.38. Student t tests indicate that the slope of the IAPs versus pH for all 25°C samples is not significantly different from zero at the 95% confidence level ($t = -0.74$, $df = 11$ for all samples). An F test indicates that the variance in log IAP values between samples is significantly different from the variance in the replicate values at the 95% confidence level ($F = 23.9$; $df_1 = 12$; $df_2 = 21$). Thus, the factors influencing such variability were more closely controlled within a given set of replicates than between samples. The charge balance errors for the "dissolution" samples range

Table 4
Calculated activities and IAPs for the chromate hydrocalumite phase in the temperature-dependent experiments

Sample batch	Measured pH	log $\{Ca^{+2}\}$	log $\{Al(OH)_4^-\}$	log $\{CrO_4^{2-}\}$	log $\{OH^-\}$	log $\{Na^+\}$	Ionic strength (m)	Charge balance error (%)[a]	Log (IAP)
5°-10.5	11.79 ± 0.04	−2.68	−2.79	−2.97	−2.89	−3.34	0.0117	3.71	−30.83 ± 0.01
5°-10.5r	11.98 ± 0.03	−2.75	−3.00	−3.07	−2.73	−3.17	0.0098	2.98	−30.77 ± 0.22
5°-11.5	12.29 ± 0.06	−2.88	−3.33	−2.98	−2.39	−2.49	0.0117	±4.07	−30.95 ± 0.18
15°-10.5	11.64 ± 0.02	−2.71	−2.97	−2.96	−2.70	−3.10	0.0116	±0.82	−30.58 ± 0.12
15°-11.5	11.89 ± 0.03	−2.79	−3.31	−2.88	−2.44	−2.49	0.0138	±0.93	−30.53 ± 0.17
35°-10.5	10.95 ± 0.02	−2.61	−2.88	−2.85	−2.73	−3.36	0.0148	2.14	−29.98 ± 0.48
35°-11.5	11.11 ± 0.05	−2.76	−3.16	−2.71	−2.57	−2.40	0.0169	1.38	−30.34 ± 0.13
45°-10.5	10.57 ± 0.04	−2.54	−2.71	−2.76	−2.93	−3.32	0.0184	5.03	−30.06 ± 0.27
45 ± -11.5	11.30 ± 0.06	−2.90	−3.29	−2.79	−2.10	−2.00	0.0216	±2.52	−29.36 ± 0.13
60°-10.5	10.15 ± 0.01	−2.55	−2.74	−2.85	−2.82	−3.16	0.0172	10.03	−29.84 ± 0.03
60°-11.5	10.53 ± 0.10	−2.70	−2.94	−2.84	−2.44	−2.37	0.0175	6.98	−29.30 ± 0.40
75°-10.5	9.90 ± 0.03	−2.61	−2.64	−2.80	−2.69	−3.14	0.0178	±2.97	−29.27 ± 0.08
75°-11.5	10.03 ± 0.02	−2.75	−2.80	−2.76	−2.56	−2.37	0.0175	2.19	−29.65 ± 0.04

[a] Charge balance error

$$= \frac{\sum_{\text{cations}} z_i c_i - \sum_{\text{anions}} z_j c_j}{\sum_{\text{cations}} z_i c_i + \sum_{\text{anions}} z_j c_j} \times 100$$

Positive values indicate excess cations, negative values indicate excess anions; ± indicates both excess cations and anions within sample replicates.

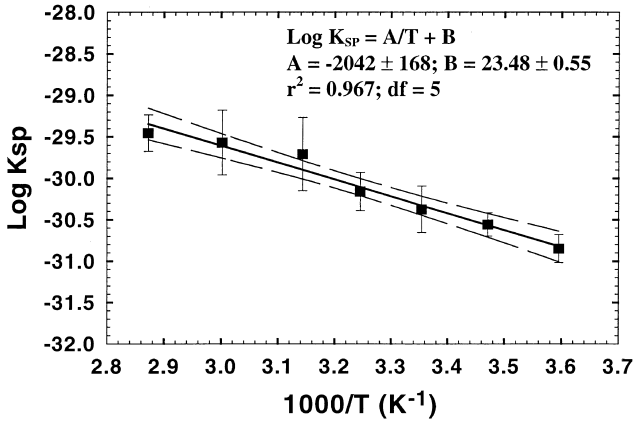

Fig. 4. Log K_{SP} versus inverse temperature. The dashed lines are the 95% confidence intervals and the vertical bars are the standard deviations in the log K_{SP} for each temperature.

from < 1% to 9% (Table 3). Activities for two of the seven "dissolution" samples (postprecipitation samples) were calculated by estimating [NO_3^-] based on minimizing the charge balance errors. The average value of charge balance errors, excluding these samples, is 3.4%. The charge balance errors for "precipitation" samples ranged from < 1% to 7.5%, with an average value of 2.3%.

The average log IAP obtained from the means of both "dissolution" and "precipitation" experiments is -30.38 ± 0.28. The error is the total standard deviation (T.S.D.), representing the error in both samples and replicates. It must be emphasized that "dissolution" and "precipitation" refer to the chromate ettringite. Because the chromate hydrocalumite formed as a secondary solid, all of the experiments are precipitation experiments with respect to this phase.

4.4. Temperature-dependent experiment

The calculated log IAPs increase with increasing temperature, ranging from -30.83 ± 0.01 at 5°C to -29.65 ± 0.04 at 75°C (Table 4). Thus, a positive enthalpy of reaction, ΔH_r°, for the dissolution of chromate hydrocalumite is indicated. The dependence of log IAP on the inverse of the temperature (Fig. 4) appears to be linear ($r^2 = .967$, $df = 5$), suggesting that the enthalpy of reaction, ΔH_r°, is constant over the temperature range 5–75°C. Using the constant enthalpy model, the $K_{SP}(T)$ can be written as

$$\log K_{SP} = \left(\frac{A}{T}\right) + B \quad (6)$$

where $A = -\Delta H_r^\circ/(\ln(10)R)$ and $B = \Delta S_r^\circ/(\ln(10)R)$. The regression coefficients obtained from fitting our data to Eq. (6) are $A = -2042.07 \pm 167.75K$ and $B = -23.48 \pm 0.55$. The log K_{SP} values calculated using these linear regression coefficients were within one standard error of the measured K_{SP} values, with the largest residual value being 0.19 for the 45°C samples.

The temperature-dependent data were also fit to a constant heat capacity model [20]. The resulting coefficients were not significant (t values < 1 at the 5% significance level), implying that this model or more complicated models, such as the variable heat capacity model, are over parameterized and inappropriate for our solubility data. Therefore, the constant enthalpy model best represents the temperature dependence of the log K_{SP} over the temperature range of 5–75°C.

4.5. Thermodynamic properties of $3CaO{\cdot}Al_2O_3{\cdot}CaCrO_4{\cdot}15H_2O$

The free energy of reaction is related to the K_{SP} by

$$\Delta G_r^\circ = -RT\ln K_{SP} \quad (7)$$

where R is the gas constant (8.31441 J mol^{-1} K^{-1}) and T is the temperature (K). Using Eq. (7) and the log K_{SP} value of -30.38 ± 0.28 calculated as the mean IAP of all 25°C experiments, we calculate $\Delta G_{r,298}^\circ = 173.4 \pm 3.7$ kJ mol^{-1}. Using this value, the free energies of formation of the individual ions presented in Table 5 and

$$\begin{aligned}\Delta G^\circ_{f,298,\text{monochromate}} = {} & 4\Delta G^\circ_{f,298}(Ca^{+2}) \\ & + 2\Delta G^\circ_{f,298}(Al(OH)_4^-) \\ & + \Delta G^\circ_{f,298}(CrO_4^{-2}) \\ & + 4G^\circ_{f,298}(OH^-) \\ & + 9\Delta G^\circ_{f,298}(H_2O) - \Delta G^\circ_{r,298}\end{aligned} \quad (8)$$

we calculate $\Delta G^\circ_{f,298} = -9905 \pm 16$ kJ mol^{-1}. The

Table 5
Formation parameters used in this study

Species	kJ mol^{-1}		J mol^{-1} K^{-1}		Refs.
	ΔG_f°	ΔH_f°	ΔS_f°	$\Delta C_{P,f}^\circ$	
H_2O_{liquid}	-237.14 ± 0.04	-285.83 ± 0.4	69.95 ± 0.03	75.351 ± 0.08	[21]
OH^-	-157.3 ± 2.0	-230.02 ± 0.6	-10.7 ± 1.9	-137.2 ± 16.7	[22][a]
Ca^{2+}	-552.79 ± 2.0	-543 ± 0.6	-56.48 ± 1.9	-31.5 ± 16.7	[22][a]
CrO_4^{2-}	-724.2 ± 1.0	-879 ± 1.0	5.4 ± 0.5	-261.9 ± 16.7	[23][b]
$Al(OH)_4^-$	-1305 ± 2.0	-1502.8 ± 1.6	101.5 ± 10	89.6 ± 12	[24]
$Ca_6[Al(OH)_6]_2(CrO_4)_3{\cdot}26H_2O$	-15131 ± 19	-17330 ± 15	2190 ± 110	2120 ± 530	[14]
$3CaO{\cdot}Al_2O_3{\cdot}CaCrO_4{\cdot}15H_2O$	-9905 ± 15.7	-11303 ± 8.3	1439 ± 89	–	This Study

[a] Uncertainties are based on maximum values reported by Shock et al. [22] over the temperature range of 0°C to 100°C.
[b] $\Delta C_{P,f}^\circ$ from Shock et al. [22].

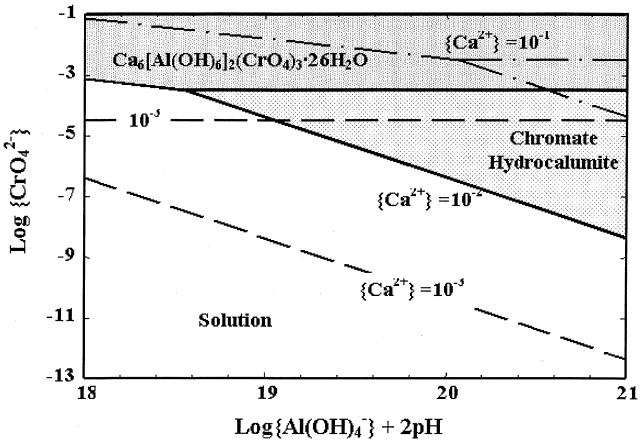

Fig. 5. Stability diagram for $Ca-Al-CrO_4^{2-}-H_2O$ system at 25°C assuming unit activity of water. The numbers on the lines denote the activity of Ca^{2+} in solution: solid lines are for stability fields for $\{Ca^{2+}\}=10^{-2}$; dashed lines for $\{Ca^{2+}\}=10^{-1}$; dash–dot lines for $\{Ca^{2+}\}=10^{-3}$.

uncertainty is based on propagation of the error associated with the K_{SP} value and the maximum possible errors associated with the free energies of the individual ions.

The enthalpy of reaction, ΔH_r°, calculated from the slope of the regression curve ($A=-2042.07\pm167.75K$) using $\Delta H_r^\circ=-A\ \ln(10)R$ is 39.1 ± 3.2 kJ mol^{-1}. The entropy of reaction, ΔS_r°, calculated from the intercept of the regression curve ($B=-23.48\pm0.55$) using $\Delta S_r^\circ=B\ \ln(10)R$ is -450 ± 10 J mol^{-1} K^{-1}. The errors are based on the standard errors of the regressed slope and intercept.

Using the data in Table 5 and equations for ΔH_f° and ΔS° analogous to Eq. (8), we calculate the enthalpy and entropy of formation of chromate hydrocalumite to be $\Delta H_f^\circ=-11303\pm8.3$ kJ mol^{-1} and $\Delta S^\circ=1439\pm89$ J mol^{-1} K^{-1}. The errors are based on the errors calculated for the dissolution reaction parameters and the maximum calculated errors associated with individual ions. A similar calculation of heat capacity resulted in $\Delta C_{Pf,298}^\circ=373\pm485$ J mol^{-1} K^{-1}. This value is not significantly different than zero.

4.6. Stability range for chromate hydrocalumite

Based on the log K_{SP} values calculated for chromate hydrocalumite and chromate ettringite we can determine conditions under which these phases are stable. Based on analogy with the sulfate system, it is likely that chromate hydrocalumite controls the solubility of Cr(VI) in mature cements. The transition is given by Eq. (9)

$$Ca_6[Al(OH)_6]_2(CrO_4)_3\cdot 26H_2O \rightleftarrows 3CaO\cdot Al_2O_3\cdot CaCrO_4\cdot 15H_2O + 2Ca^{2+} + 2CrO_4^{2-} + 17H_2O. \quad (9)$$

At equilibrium, this transformation can be expressed as

$$\log K_{Cr(VI)-ettringite} - \log K_{chromate\ hydrocalumite} \rightleftarrows 2\log Ca^{2+} + 2\log CrO_4^{2-} + 17\log H_2O \quad (10)$$

where $K_{chromate\ hydrocalumite}$ and $K_{Cr(VI)\text{-}ettringite}$ are the solubility products for the reactions given by Eq. (4) and by

$$Ca_6[Al(OH)_6]_2(CrO_4)_3\cdot 26H_2O \rightleftarrows 6Ca^{2+} + 2Al(OH)_4^- + 3CrO_4^{2-} + 4OH^- + 26H_2O, \quad (11)$$

respectively. Using the values of the solubility products at 25°C (log $K_{SP,Cr(VI)\text{-}ettringite}=-41.5\pm0.3$) and Eqs. (5), (10), and (11), we generated the stability diagram in Fig. 5. The solid lines denote the stability regions when $\{Ca^{2+}\}=10^{-2}$. When $\{Ca^{2+}\}$ increases to 10^{-1}, the stability region for chromate hydrocalumite increases in size and the resulting Cr(VI) concentrations are much lower. When $\{Ca^{2+}\}$ decreases to 10^{-3}, the stability region for chromate hydrocalumite decreases in size and the resulting Cr(VI) concentrations are much higher.

The solubility products for both chromate hydrocalumite and the Cr(VI)-analog of ettringite are temperature dependent and the stability regions therefore shift with temperature (Fig. 6). The stability region for chromate hydrocalumite is small at 5°C and becomes relatively large at 75°C. There is, however, very little shift in the boundary between $Ca_6[Al(OH)_6]_2(CrO_4)_3\cdot 26H_2O$ and $3CaO\cdot Al_2O_3\cdot CaCrO_4\cdot 15H_2O$ with temperature. These results indicate that consideration of the temperature of the system is important in determining the stability of these phases in concrete.

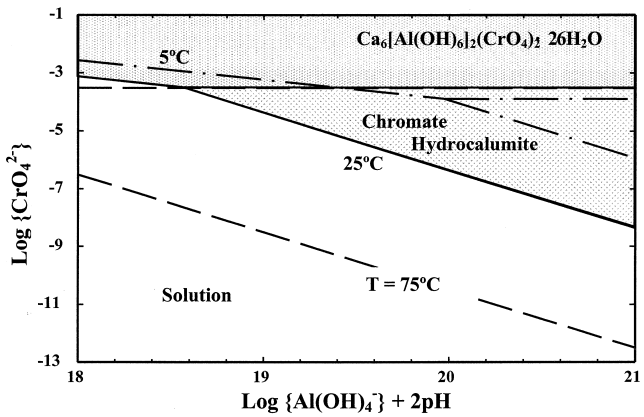

Fig. 6. Stability diagram for $Ca-Al-CrO_4^{2-}-H_2O$ system assuming unit activity of water and $\{Ca^{2+}\}=10^{-3}$. The numbers on the line denote the temperature: solid lines denote 25°C; dash–dot lines denote 75°C; dashed lines denote 5°C.

5. Summary

Powder XRD of solids present in a reactor at the end of dissolution and precipitation experiments using a Cr(VI) analog of ettringite revealed the presence of a secondary phase. This precipitate was identified as the Cr(VI) analog of sulfate hydrocalumite (monosulfate). The solubility product of $3CaO{\cdot}Al_2O_3{\cdot}CaCrO_4{\cdot}15H_2O$ for Eq. (4) at 25°C was calculated to be -30.38 ± 0.28. Experiments conducted over the temperature range of 5–75°C indicate that the enthalpy and entropy of reaction are 39.1 ± 3.2 kJ mol^{-1} and -450 ± 10 J mol^{-1} K^{-1}, respectively. The free energy of formation and enthalpy of chromate hydrocalumite calculated from our results and published partial molal quantities for key ions are -9905 ± 16 and -11303 ± 8.3 kJ mol^{-1}. $\Delta S°$ is calculated to be 1439 ± 89 J mol^{-1} K^{-1}.

References

[1] F.M. Lea, The Chemistry of Cement and Concrete, third ed., Edward Arnold, Glasgow, 1970, 727 pp.

[2] I. Odler, S. Abdul-Maula, Possibilities of quantitative determination of the AFt-(ettringite) and AFm-(monosulphate) phases in hydrated cement pastes, Cem. Concr. Res. 14 (1984) 133–141.

[3] E.T. Carlson, H.A. Berman, Some observations on the calcium aluminate carbonate hydrates, J. Res. Natl. Bur. Stand., Sect. A, Phys. Chem. 64 (4) (1960) 333–341.

[4] H. Poellman, S. Auer, H.J. Kuzel, R. Wenda, Solid solution of ettringites: Part II. Incorporation of $B(OH)_4^-$ and CrO_4^{2-} in $Ca_6Al_2O_6(SO_4)^3{\cdot}32H_2O$, Cem. Concr. Res. 23 (1993) 422–430.

[5] H. Poellman, H.J. Kuzel, R. Wenda, Solid solution of ettringites: Part I. Incorporation of OH^- and CO_3^{2-} in $3CaO{\cdot}Al_2O_3{\cdot}3CaSO_4{\cdot}32H_2O$, Cem. Concr. Res. 20 (1990) 941–947.

[6] E.J. Reardon, An ion interaction model for the determination of chemical equilibria in cement/water systems, Cem. Concr. Res. 20 (1990) 175–192.

[7] M. Zhang, Incorporation of oxyanionic B, Cr, Mo, and Se into hydrocalumite and ettringite: Application to cementitious systems, Dissertation, University of Waterloo, Waterloo, Ontario, Canada, 1995, 171 pp.

[8] E. Nieboer, S.L. Shaw, in: J.O. Nriagu, E. Nieboer (Eds.), Chromium in the Natural and Human Environments, Mutagenic and other genotoxic effects of chromium compounds, Wiley, New York, 1988, pp. 399–437.

[9] G.F. Nordberg, Current concepts in the assessment of effects of metals in chronic low-level exposures; considerations of experimental and epidemiological evidence, Sci. Total Environ. 71 (1988) 243–252.

[10] P. O'Brien, A. Kortenkamp, Chemical models important in understanding the ways in which chromate can damage DNA, Environ. Health Perspect. 102 (Suppl. 3) (1994) 3–10.

[11] M. Sugiyama, Role of paramagnetic chromium in chromium (VI)-induced damage in cultured mammalian cells, Environ. Health Perspect. 102 (Suppl. 3) (1994) 31–33.

[12] C.D. Palmer, Precipitates in a Cr(VI)-contaminated concrete, Environ. Sci. Technol. 34 (2000) 4185–4192.

[13] H.-J. Kuzel, Initial hydration reactions and mechanisms of delayed ettringite formation in Portland cements, Cem. Concr. Compos. 18 (3) (1996) 195–203.

[14] R.B. Perkins, C.D. Palmer, Solubility of $Ca_6[Al(OH)_6]_2(CrO_4)_3-26H_2O$, the chromate analog of ettringite; 5–75°C, Appl. Geochem. 15 (2000) 1203–1218.

[15] APHA, in: M.H. Franson (Ed.), Standard Methods for the Examination of Water and Wastewater, American Public Health Association, Washington, DC, 1995, 1100 pp.

[16] J.I. Goldstein, D.E. Newbury, P. Echliln, D.C. Joy, A.D. Romig, C.E. Lyman, C. Fiori, E. Lifshin, Scanning Electron Microscopy and X-ray Microanalysis, Plenum, New York, 1992, 820 pp.

[17] S.C.B. Myneni, Oxyanion–mineral surface interactions in alkaline environments: AsO_4 and CrO_4 sorption and desorption in ettringite, Dissertation, The Ohio State University, 1995, 250 pp.

[18] H.Y. Ghorab, E.A. Kishar, Studies of the stability of the calcium sulfoaluminate hydrates: Part I. Effect of temperature on the stability of ettringite in pure water, Cem. Concr. Res. 15 (1985) 93–99.

[19] J.D. Allison, D.S. Brown, K.J. Novo-Gradac, MINTEQA2/PRODEFA2, a geochemical model for environmental systems: Version 3.0, U.S. Environmental Protection Agency, 1990.

[20] D.K. Nordstrom, J.L. Munoz, Geochemical Thermodynamics, second ed., Blackwell Scientific Publications, Boston, MA, 1994, 493 pp.

[21] J.D. Cox, D.D. Wagman, V.A. Mededev, CODATA Key Values for Thermodynamics, Hemisphere Publishing, 1989, 271 pp.

[22] E.L. Shock, D.C. Sassani, M. Willis, D.A. Sverjensky, Inorganic species in geologic fluids: Correlations among standard molal thermodynamic properties of aqueous ions and hydroxide complexes, Geochim. Cosmochim. Acta 61 (5) (1997) 907–950.

[23] J.W. Ball, D.K. Nordstrom, Critical evaluation and selection of standard state thermodynamic properties for chromium metal and its aqueous ions, hydrolysis species, oxides, and hydroxides, J. Chem. Eng. Data 43 (6) (1998) 895–918.

[24] K. Nordstrom, H.M. May, in: G. Sposito (Ed.), The Environmental Chemistry of Aluminum, Aqueous equilibrium data for mononuclear aluminum species, Lewis Publishers, Boca Raton, FL, 1996, pp. 39–80.

[25] B.S. Hemingway, G. Sposito, in: G. Sposito (Ed.), The Environmental Chemistry of Aluminum, Inorganic aluminum-bearing solid phases, CRC Press, Boca Raton, FL, 1996, pp. 81–116.

[26] D.P. Garvin, V.B. Parker, H.J. White, CODATA Thermodynamic Tables — Selections for Some Compounds of Calcium and Related Mixtures: A Prototype Set of Tables, Hemisphere Publishing, 1987, 365 pp.

[27] D.K. Nordstrom, L.N. Plummer, D. Langmuir, E. Busenberg, H.M. May, B.F. Jones, D.L. Parkhurst, Revised chemical equilibrium data for major water–mineral reactions and their limitations, Chemical Modeling of Aqueous Systems II: ACS Symposium Series, American Chemical Society, Washington, DC, 1990, pp. 398–413.